Published in final edited form as:

Science. 2018 December 21; 362(6421): . doi:10.1126/science.aan3303.

E-C coupling structural protein junctophilin-2 encodes a stress-adaptive transcription regulator

Ang Guo[1], **Yihui Wang**[1,2], **Biyi Chen**[1], **Yunhao Wang**[1], **Jinxiang Yuan**[1], **Liyang Zhang**[3], **Duane Hall**[1], **Jennifer Wu**[1], **Yun Shi**[1], **Qi Zhu**[1,4], **Cheng Chen**[1,2], **William H. Thiel**[1], **Xin Zhan**[1], **Robert M. Weiss**[1], **Fenghuang Zhan**[1], **Catherine A. Musselman**[3], **Miles Pufall**[3], **Weizhong Zhu**[4], **Kin Fai Au**[1], **Jiang Hong**[2], **Mark E. Anderson**[5], **Chad E. Grueter**[1,6], and **Long-Sheng Song**[1,6,7,*]

[1]Department of Internal Medicine, Abboud Cardiovascular Research Center, Carver College of Medicine, University of Iowa, Iowa City, IA 52242, USA

[2]Department of Emergency Medicine, Shanghai General Hospital, Shanghai Jiao Tong University School of Medicine, Shanghai 200080, China

[3]Department of Biochemistry, Carver College of Medicine, University of Iowa, Iowa City, IA 52242, USA

[4]Department of Pharmacology, School of Pharmacy, Nantong University, 19 Qixiu road, Nantong, Jiangsu 226001, China

[5]Department of Medicine, Johns Hopkins School of Medicine, Baltimore, MD 21205, USA

[6]Fraternal Order of Eagles Diabetes Research Center, Carver College of Medicine, University of Iowa, Iowa City, IA 52242, USA

[7]Iowa City Veterans Affairs Medical Center, Iowa City, IA 52242, USA

Abstract

Junctophilin-2 (JP2) is a structural protein required for normal excitation-contraction (E-C) coupling. Following cardiac stress, JP2 is cleaved by Ca^{2+}-dependent protease calpain, which disrupts the E-C coupling ultrastructural machinery and drives heart failure progression. Here we demonstrate that stress-induced proteolysis of JP2 liberates an N-terminal fragment (JP2NT) that translocates to the nucleus, binds to genomic DNA and controls expression of a spectrum of genes in cardiomyocytes. Transgenic overexpression of JP2NT in mice modifies the transcriptional

*Correspondence to: Long-Sheng Song, M.D., Department of Internal Medicine, Abboud Cardiovascular Research Center, Carver College of Medicine, University of Iowa, Iowa City, IA 52242, USA. long-sheng-song@uiowa.edu; Telephone: (319) 384-2890 (office); Fax: (319) 353-5552.

Present address: Kin Fai Au, Department of Biomedical Informatics, Ohio State University, Columbus, OH 43210.

Author contributions: L.S.S. supervised the project; A.G. and L.S.S. designed the study; A.G., Y.W., B.C., J.Y., L.Y.Z., D.H., J.W., Y.S., Q.Z., C.C., R.W., X.Z. performed the experiments and data analysis; Y.W. (Yunhao) and A.G. performed bioinformatics analyses; C.G., M.E.A, F.Z., K.F.A., C.M., M.P., W.Z. and J.H. participated in supervision of experiments, data analysis, interpretations and revision of the manuscript. A.G. and L.S.S. wrote the manuscript. All authors reviewed the results, edited and approved the final version of the manuscript.

Competing interests: The authors have no conflicting financial interests.

Data and materials availability: Microarray and Sequencing data are available at NCBI Gene Expression Omnibus (GEO) with accession numbers (GSE121545, GSE121546, GSE121547). All other data are available in the manuscript or the supplementary materials.

profile resulting in attenuated pathological remodeling in response to cardiac stress. Conversely, loss of JP2NT function accelerates stress-induced development of hypertrophy and heart failure in mutant mice. These data reveal a self-protective mechanism in failing cardiomyocytes that transduce mechanical information (E-C uncoupling) into salutary transcriptional reprogramming in the stressed heart.

One Sentence Summary:

JP2, an integral structural protein important for E-C coupling, contains a conserved DNA binding domain that regulates transcriptional pathways and confers cardiac protection against stress.

Ca^{2+} signaling affects almost every aspect of cells from life to death (1). In heart muscle, excitation-contraction (E-C) coupling is a cascade of Ca^{2+}-mediated processes linking membrane depolarization to activation of cell contraction (2). At the cellular level, E-C coupling in working ventricular myocytes depends on precise communication between voltage-gated L-type Ca^{2+} channels located mainly on the transverse (T)-tubule membrane and Ca^{2+}-sensitive ryanodine receptors (RyRs) on the terminal cisternae of the sarcoplasmic reticulum (SR) (3–6). Upon membrane depolarization, Ca^{2+} influx through the opening of voltage-gated L-type Ca^{2+} channels increases [Ca^{2+}] locally. This high concentration of [Ca^{2+}] sensitizes adjacent RyRs to release a much larger amount of Ca^{2+} from the SR. The SR-released Ca^{2+} together with Ca^{2+} influx activates myofilaments, resulting in myocyte contraction. This intermolecular Ca^{2+} crosstalk between L-type Ca^{2+} channels and RyRs takes place in a confined spatial microdomain, where T-tubules and terminal cisternae of SR form tight junctional couplings with a gap of 12-15 nm, termed “cardiac dyads” (7). Cardiac dyads provide the structural basis for E-C coupling and are established and maintained by junctophilin-2 (JP2) (8). JP2 contains eight N-terminal ‘membrane occupation and recognition nexus’ (MORN) domains that mediate interactions with the T-tubule membrane, a space-spanning α-helix which is thought to control the dyad distance, and a C-terminal transmembrane (TM) domain that anchors JP2 in the SR membrane (8, 9). Genetic manipulation of JP2 by silencing, knockout or overexpression authenticated its role as a structural protein responsible for the formation of cardiac dyads and maintenance of normal E-C coupling in the heart (8, 10, 11).

Defective E-C coupling is a hallmark of heart failure (12–16). Recent studies have provided compelling evidence that the expression level of JP2 is decreased in failing hearts of multiple etiologies including human heart failure, contributing to the loss of ultrastructural integrity of cardiac dyads and E-C coupling dysfunction (16–22). In particular, we discovered that JP2 proteolytic cleavage by calpain in response to cardiac stress represents a key mechanism of JP2 downregulation, causing E-C uncoupling, Ca^{2+} mis-handling, and heart failure (23–25). Abnormal Ca^{2+} homeostasis triggers maladaptive transcriptional remodeling, contributing to pathological myocardial remodeling and development of heart failure (26–32). However, it was not clear whether cardiomyocytes undergoing E-C uncoupling possess a self-protective or homeostatic mechanism that mitigates adverse myocardial remodeling. It was also unknown whether there is an intrinsic connection between cardiac ultrastructural remodeling at E-C coupling junctions and transcriptional reprogramming in stressed hearts. Here we show a mechanism in which a JP2 fragment,

generated during cardiac stress and a marker of E-C uncoupling, serves as a negative feedback mechanism to antagonize maladaptive cardiac remodeling. This fragment translocates to the nucleus and represses transcriptional reprogramming, in part through regulating a key muscle transcription factor MEF2. Specifically, we found the α-helix domain of JP2 contains an evolutionarily conserved DNA binding domain. Under stress conditions, proteolytic processing of JP2 by calpain converts it from a structural protein to a transcriptional regulator, indicating an intrinsic connection between cardiomyocytes ultrastructural remodeling and transcriptional reprogramming in the heart.

Nuclear localization of JP2NT

We previously reported that JP2 is a substrate of calpain and identified the primary calpain proteolysis site in the C-terminal region of JP2 between residues R^{565}/T^{566} (24). Calpain cleavage creates an N-terminal truncate (residues 1-565, termed “JP2NT”) that contains the plasma membrane-binding MORN motifs, and a C-terminal fragment containing the SR membrane-anchoring TM domain (Fig. 1A). We performed western blotting with an antibody against an internal epitope of JP2, which is not destroyed by calpain cleavage of JP2 (fig. S1A). Analysis of subcellular fractions of mouse myocardium established that endogenous JP2NT (75KD) is present and predominantly enriched in nuclear fractions (Fig. 1B fig. S1B&C). Immunostainings of human and mouse myocardium sections using the same antibody also detected a JP2 product in nuclei (denoted by arrows in fig. S2). In contrast, an antibody against the C-terminus of JP2 didn’t detect JP2 signals in the nucleus of myocardium sections (fig. S2). JP2NT was dramatically increased in myocardium from mice with cardiac-specific overexpression of calpain 1 and enriched in the nuclear fraction (Fig. 1C) (for calpain1-OE mice, see (33)). In addition, treatment with micrococcal nuclease (MNASE), which cleaves DNA and releases chromatin-associated proteins, released JP2NT from the chromatin pellet (Fig. 1C), substantiating the nuclear localization of endogenous JP2NT *in vivo* and also suggesting that JP2NT is a chromatin-associated protein.

We hypothesized that pathological stresses that activate calpain (34) promotes the generation and nuclear accumulation of JP2NT. Consistent with this notion, we found both isoproterenol infusion (Fig. 1D, fig. S1B & S2A) and myocardial infarction (Fig. 1E, fig. S1C, S2B&C) increased the amount of JP2NT in nuclei of stressed hearts compared with (sham) controls. Under pressure overload stress, nuclear accumulation of JP2NT reached its peak at 2~3 weeks after transaortic banding (TAB) surgery (Fig. 1F). Conversely, administration of the calpain inhibitor MDL-28170 significantly attenuated stress-induced elevation in nuclear JP2NT (Fig. 1D-F), further supporting that calpain-mediated proteolysis of full-length JP2 under cardiac stress results in accumulation of nuclear JP2NT.

These data led us to postulate that the posttranslational removal of JP2 C-terminus is sufficient to promote JP2NT translocation into the nucleus. To recapitulate the process by which calpain-mediated proteolysis is associated with JP2NT translocation, we adapted an inducible split tobacco etch virus protease (sTEVp) system (Fig. 1G-a) (35). A TEVp substrate recognition sequence (TRS) was inserted into eGFP-JP2 in the primary calpain cleavage site (R^{565}/T^{566}) (eGFP-JP2TRS, Fig. 1G-a). At baseline in HEK293T cells, eGFP-JP2TRS was localized at the cell membrane and an intracellular network-like structure that

is likely the endoplasmic reticulum (Fig. 1G-b). In the absence of rapamycin, co-transfection of sTEVp did not affect eGFP-JP2TRS localization (Fig. 1G-c). In cells expressing sTEVp, rapamycin treatment rapidly and dramatically induced nuclear importation of eGFP-JP2TRS N-terminus (Fig. 1G-e). These data show that JP2 c-terminus anchors the intact JP2 protein at the dyad, and removal of JP2 C-terminus is sufficient to induce trafficking of the N-terminal fragment into nuclei.

JP2NT has a NLS and a chromatin/DNA binding region

To investigate the molecular mechanism of JP2NT nuclear importation, we performed an *in silico* analysis (36). In JP2NT, we found a monopartite **n**uclear **l**ocalization **s**ignal (NLS), $K^{488}RPRP^{492}$ and a bipartite **NLS**-like peptide (bNLS), $K^{345}RRVLPLKSSKVRQK^{359}$, adjacent to an **a**lanine-**r**ich **r**egion (ARR, A^{367}-A^{402}) (fig. S3A), that shows characteristics of a helix-turn-helix structure (GYM 2.0 (37)). These domains are evolutionarily conserved among species (fig. S3B&C). Fusion of a short peptide containing this monopartite NLS to mCherry resulted in nuclear enrichment of the fusion proteins (fig. S3D). Deletion of this sequence ($JP2NT^{\Delta NLS}$) abolished nuclear localization of eGFP-JP2NT in HEK293T cells (Fig. 2A-c-d) and cardiomyocytes (fig. S3E), indicating this NLS is indispensable for nuclear localization of JP2NT. A fusion protein containing mCherry and the bNLS peptide together with the ARR was imported into nuclei (fig. S3D). However, deletion of the bNLS sequence from JP2NT (eGFP-$JP2NT^{\Delta bNLS}$) did not prevent its nuclear importation in HEK293T cells (Fig. 2A-e) and cardiomyocytes (fig. S3E), indicating that this region is not necessary for nuclear importation of JP2NT. However, the sub-nuclear localization of eGFP-$JP2NT^{\Delta bNLS}$ was mutually exclusive from To-Pro-3 staining, which labels genomic DNA (Fig. 2A-e), suggesting physical dissociation of eGFP-$JP2NT^{\Delta bNLS}$ from genomic DNA. Deletion of the adjacent ARR from JP2NT (eGFP-$JP2NT^{\Delta ARR}$) induced greater separation of eGFP-JP2NT from DNA and was accompanied by accumulation of DNA at the nuclear periphery (Fig. 2A-f). These data indicate that bNLS and ARR are involved in DNA or chromatin binding.

To further confirm the association of JP2NT with chromatin, we applied a biochemical fractionation procedure (38) (Fig. 2B-a). JP2NT was detected in both soluble (S3) and chromatin-containing insoluble (P4) nuclear fractions (Fig. 2B-b-i). MNASE-mediated DNA digestion released JP2NT from the insoluble chromatin fraction (MNASE+ / S4) (Fig. 2B-b-i). Deletion of the 8 MORN domains from JP2NT ($JP2NT^{\Delta MORNs}$) did not influence its distribution in the nucleus or its association with chromatin (Fig. 2B-b-ii). In contrast, deletion of the bNLS-like signal from this construct ($JP2NT^{\Delta MORNs/\Delta bNLS}$) significantly reduced the association of JP2NT with chromatin (Fig. 2B-b-iii). Deletion of the alanine-rich domain in combination with the bNLS ($JP2NT^{\Delta MORNS/\Delta bNLS/\Delta ARR}$ or $JP2NT^{\Delta bNLS/\Delta ARR}$) completely prevented localization of JP2NT in the MNASE-releasable chromatin fraction (Fig. 2B-b-iv~vi). Based on these data, we conclude that JP2NT associates with chromatin via a domain located at residues ~345-402, which is highly evolutionarily conserved in mammalian species as well as in vertebrate such as fish and birds (fig. S3C).

JP2NT is enriched at transcription start sites

To systematically study the genomic targets of JP2NT, we generated transgenic mice with cardiac-specific overexpression of HA-tagged JP2NT. In these mice, JP2NT is predominantly localized in the nuclei of cardiomyocytes (fig. S4A). The level of JP2NT transgene in nuclear fraction is in the same order of magnitude, compared to the peak level of endogenous JP2NT induced by TAB (Fig. 1F). Hearts of the JP2NT overexpressing mice (JP2NT-OE) were subjected to ChIP-seq analysis using anti-HA antibody. Two replicates of ChIP-Seq analyses were performed using different batches of JP2NT heart samples. Only the DNA peaks ($p<10^{-10}$) that were detected in both replicates of ChIP-seq analyses were considered as JP2NT-binding DNA regions. We identified 9414 JP2NT-binding genomic DNA regions encompassing 7398 genes. The DNA binding profile revealed that JP2NT is concentrated in gene-enriched regions, especially the promoter and 5' UTR regions (Fig. 3A). Moreover, JP2NT is preferentially enriched at transcription start sites (TSS) (Fig. 3B), a characteristic of transcription regulators. We compared JP2-NT occupancy of genomic loci with that of cardiac Pol II and H3K9ac binding peaks from published data (39). We found that 95% of JP2NT peaks overlap with H3K9ac (a marker for active promoters and enhancers) peaks, and 78% overlap with Pol II peaks (Fig. 3C, example tracks shown in fig. S4B-a). These data strongly suggest that JP2NT regulates active cardiac transcription.

JP2NT is a TATA box binding protein and interacts with transcription machinery

Based on these results, we hypothesized that JP2NT may directly associate with core cis-regulatory elements that regulate transcription initiation. Crosslinking-reversal co-IP experiments in JP2NT transgenic cardiomyocytes demonstrated that JP2NT associates with RNA polymerase II (RPB1) and TATA-box binding protein (TBP), both of which are components of the basic transcriptional machinery (fig. S5A). TBP specifically binds to TATA boxes, eukaryotic core cis-regulatory elements localized at TSS. Subsequent *in vitro* analysis with purified recombinant GST-JP2NT revealed that JP2NT directly binds to the TATA box or variants (TATAAA, TATAAT and TATATA) from the cMyc (Fig. 3D-a *and* fig. S5B) or the CMV promoter (fig. S5C). This interaction was abrogated by mutation of the TATA box elements (Fig. 3D-b and fig. S5B). We conclude that JP2NT is a DNA binding protein, binding to consensus TATA box represented as TATAA(A/T) or TATATA (Fig. 3D-c).

Deletion of N-terminal MORN domains alone from JP2NT (GST-JP2NT$^{\Delta MORNs}$) did not alter the interaction of JP2NT with the TATA box oligonucleotide (Fig. 3D-d and fig. S5C). However, deletion of the ARR from this construct (GST-JP2NT$^{\Delta MORNs/\Delta ARR}$) completely abrogated the association of JP2NT with TATA box elements (Fig. 3D-d and fig. S5C). Conversely, a purified peptide containing the ARR (GST-JP2$^{331\text{-}405}$) specifically bound to the consensus but not mutant TATA box (Fig. 3D-e and fig. S5D). Together, these data indicate that the ARR is responsible for TATA box binding.

JP2NT modulates MEF2-mediated transcription via competing for MEF2 binding sites

The MEF2 family, master regulators of hypertrophic genes in cardiomyocytes, binds to the A/T enriched consensus sequence (*C/T* TA(A/T)4TA *G/A*), which shares the same core sequence with TATA box. Thus, we hypothesized that JP2NT directly interacts with MEF2 response element (MRE). Consistent with this hypothesis, MEF2 binding motifs were significantly enriched in the ChIP-seq dataset (Fig. 4A, Suppl_Excel_file 1). Gel shift assay demonstrated that purified JP2NT or purified DNA binding domain of JP2NT (GST-$JP2^{331\text{-}405}$) interacts with a MRE from the Desmin enhancer (Fig. 4B and fig. S6A). The specificity of this interaction was further shown by mutant MRE oligos (Fig. 4B) and cold competitor assay (fig. S6B). Biotinylated oligo DNA pull-down assay confirmed that the JP2NT transgene as well as endogenous full-length JP2 from heart lysis can interact with MRE (fig. S6C). Co-IP of HEK293T cells transfected with Myc-tagged MEF2C and HA-tagged JP2NT demonstrated an interaction of the two proteins (Fig. 4C). The interaction of endogenous MEF2C with JP2NT transgene was confirmed in JP2NT transgenic hearts (Fig. 4C).

To examine whether JP2NT regulates MEF2-mediated transcription, we utilized a luciferase reporter system with firefly cDNA driven by Desmin enhancer-derived MRE (P_{MEF2}-firefly) (40). Co-transfection of plasmid expressing MEF2C and P_{MEF2}-firefly in HEK293T cells significantly increased the firefly luciferase signal relative to constitutive P_{SV40}-renilla (Fig. 4D, E). Co-transfection of JP2NT attenuated the MEF2-responsive signal in a dose-dependent manner (Fig. 4D). By contrast, MEF2C-mediated transcriptional activity was not significantly altered in cells expressing a JP2NT construct lacking the ARR ($JP2NT^{\Delta ARR}$, Fig. 4E), which we found to be required for its association with chromatin and TATA box sequences. These data suggest that JP2NT competes with MEF2 for direct interaction with its consensus sequence at promoters to block MEF2-mediated transcription.

JP2NT alters DNA binding profiles of TBP and MEF2C in cardiomyocytes

To understand whether JP2NT influences DNA occupancy of MEF2 in cardiomyocytes, we analyzed the DNA binding profile of MEF2C in control and JP2NT-OE myocardium. ChIP-seq analyses revealed that JP2NT-OE suppressed MEF2C interactions at 42% of the endogenous MEF2C binding sites. JP2NT-OE created 2386 new MEF2C binding peaks that are absent in control hearts, and 65% of them overlap with JP2NT binding sites. In addition, 33% of the MEF2C binding peaks inhibited by JP2NT-OE overlap with JP2NT binding sites (Fig. 4F). ChIP-seq analyses of TBP revealed that ~25% of the endogenous TBP binding sites were suppressed by JP2NT-OE, and 22% of them overlap with JP2NT binding sites. JP2NT-OE created 2192 new TBP binding peaks, and 28% of them overlap with JP2NT binding sites (Fig. 4F, example tracks shown in fig. S4B-b-e). These data indicate that JP2NT can affect MEF2C and TBP DNA binding either by competing for the endogenous binding sites or by recruiting MEF2C and TBP to new binding sites.

Overexpression of JP2NT in cultured cardiomyocytes induces profound changes in transcriptional profile

The association of JP2NT with DNA and transcription machinery led us to investigate whether JP2NT directly modulates the transcriptional profile in cardiomyocytes. Compared with cardiomyocytes infected with empty adenovirus (Ad-Empty control), Affymetrix GeneChip analysis revealed that the expression of 574 and 1996 known genes were significantly induced or repressed ($p<0.01$), respectively, in JP2NT-expressing cardiomyocytes (Fig. 5 A & fig. S7A see Suppl_Excel_file 2 for complete list of differentially expressed genes). Conversely, only 96 significantly induced and 264 significantly repressed genes were detected in cardiomyocytes with overexpression of full length JP2 (Fig. 5A & fig. S7B). Importantly, ~60% of the differentially expressed genes induced by JP2NT mapped to genomic loci where JP2NT was found to bind by ChIP-seq, which is significantly larger than the percentage (~46%, $p<10^{-15}$) of JP2NT binding genes in those genes whose expression was detectable in cardiomyocytes but was not significantly influenced by JP2NT. Notably, the regulatory effect of JP2NT on gene expression appeared to be dependent on binding of JP2NT to gene loci: among the differentially expressed genes for which JP2NT bound to the genomic loci, the vast majority (84%) were down-regulated in the presence of JP2NT overexpression; this percentage is decreased to 67% ($p<10^{-15}$) in differentially expressed genes not bound by JP2NT. We interpret these findings to indicate that JP2NT represses transcription by binding to genomic regions, either directly through binding to TATA box and MRE or through interactions with transcription factors such as MEF2C and TBP.

Many of the JP2NT-downregulated genes encode nuclear proteins (fig. S7C) and proteins that are functionally enriched in nuclear events such as transcriptional regulation and chromatin modification (fig. S7D). Ingenuity Pathway Analysis (IPA) of the differentially expressed genes induced by JP2NT identified pathways and regulators implicated in cardiac hypertrophy, fibrosis, cell growth and differentiation as well as inflammation. Specifically, ERK/MAPK, NF-κB, TGF-β and integrin signaling pathways were predicted to be inhibited in response to JP2NT overexpression (Fig. 5B, See Suppl_Excel_file 3). Confirming these GeneChip findings, qPCR revealed that mRNA levels of genes including KLF4, KLF6, Myc, TGFβR1, NFKBIA, FOXO1, PI3KR1 et al, were significantly decreased in cardiomyocytes expressing JP2NT compared with Ad-Empty infected cells (Fig. 5C). Deletion of the DNA binding region from JP2NT ($JP2NT^{\Delta bNLS/\Delta ARR}$) largely prevented the repressive effect of JP2NT (Fig. 5C). Notably, the cardiac hypertrophy markers ANP and BNP were not altered by JP2NT expression but were significantly increased by $JP2NT^{\Delta bNLS/\Delta ARR}$ (Fig. 5C).

To further test whether JP2NT regulates transcription of these genes, we constructed luciferase reporters controlled by promoters of Myc, KLF6, TGFβR1, and NFKBIA. For all genes, promoter activity was significantly attenuated by co-expression of JP2NT in HEK293T cells (Fig. 5D). Consistent with the changes in mRNA levels, expression of $JP2NT^{\Delta bNLS/\Delta ARR}$ either had no effect on baseline firefly luciferase signal or increased promoter activity as compared to empty vector control (Fig. 5D), supporting that the DNA binding domain of JP2NT is important for its function as a transcriptional repressor.

JP2NT attenuates hypertrophic response and heart failure development in mice

Since JP2NT represses transcription of key regulators of hypertrophy, fibrosis, and inflammation, we predicted JP2NT would exert a protective effect on stress-induced pathological cardiac remodeling. At baseline, JP2NT overexpression had no effect on cardiac morphology or function (Fig. 6A-C). The E-C coupling function at single cell level (e.g., L-type Ca^{2+} channel densities, amplitude and kinetics of Ca^{2+} transients, SR Ca^{2+} content as well as the gain function of E-C coupling) was not altered by JP2NT transgene (fig. S8). Under stress conditions induced by TAB surgery to produce pressure overload hypertrophy and heart failure, JP2NT-OE mice had improved cardiac function (Fig. 6A), lower heart weight/body weight ratio (Fig. 6B) and reduced lung edema indicated by the lung weight/body weight ratio (Fig. 6C) relative to controls. These results suggest that JP2NT-OE protects the heart against stress-induced pathological remodeling.

RNA-Seq demonstrated minor differences in the cardiac transcription profile of JP2NT-OE mice at baseline relative to control littermates (fig. S9A), with only 220 significantly altered genes ($p<0.01$). TAB promoted a marked change in the transcriptome of control hearts as compared to sham surgery, with 4636 significantly altered transcripts derived from 3580 genes (fig. S8B). Overexpression of JP2NT significantly modified the transcriptional response to cardiac stress: we detected a significant difference in 1082 transcripts derived from 954 known genes based on a linear regression model ($p <0.01$, Fig. 6D). Among these, 540 transcripts (mapped to 481 known genes) were negatively influenced and 542 transcripts (mapped to 476 known genes) positively influenced by JP2NT overexpression (See Suppl_Excel_file 4), with a predicted inhibition of ERK, TGF-β, CREB and NF-κB signaling pathways (Fig. 6E, See Suppl_Excel_file 5). These findings are in line with observations in cultured cardiomyocytes (Fig. 5B) and substantiate a pivotal role for JP2NT in the cardiac response to stress by inhibiting transcriptional reprogramming.

Loss of function of JP2NT exacerbates cardiac dysfunction in response to stress

To investigate the function of endogenous JP2NT, we developed a knockin (KI) mouse line with NLS deleted in the JP2 coding sequence ($JP2^{\Delta NLS}$-KI) (fig. S10A). NLS deletion abolished the nuclear accumulation of JP2NT following cardiac stress (fig. S10B). The homozygous $JP2^{\Delta NLS}$-KI mice show no difference in cardiac morphology, contractile function, and cellular E-C coupling / Ca^{2+} handling function compared to WT littermates under baseline condition (Fig. 6F-I, fig. S10C-E). However, when subjected to TAB, $JP2^{\Delta NLS}$-KI mice developed more severe cardiac hypertrophy and worsened heart function relative to WT littermates. Three weeks after TAB, echocardiography detected larger myocardium mass (Fig. 6F), higher End Diastolic Volume (EDV) (Fig. 6H) and End Systolic Volume (ESV) (Fig. 6I) as well as lower ejection fraction (Fig. 6G) in $JP2^{\Delta NLS}$-KI mice than in WT littermates. These findings suggest that JP2NT functions as an endogenous cardiac protector against pathological challenges.

Discussion

Our study provides compelling evidence suggesting that an E-C coupling structural protein can also act as a transcriptional regulator. Herein we demonstrate that regulated cleavage of JP2 converts it from a structural protein to a nuclear transcriptional regulator via an NLS and an ARR contained within JP2NT. JP2NT is enriched in the promoter region of genes in cardiomyocytes and primarily acts as a transcriptional repressor of genes implicated in cell growth and differentiation, hypertrophy, inflammation and fibrosis, with evidence for a specific interaction with the transcription factor MEF2. Cardiac-specific transgenic overexpression of JP2NT attenuates pressure overload induced development of heart failure, identifying JP2NT generation as a self-protective homeostatic mechanism that safeguards against the deleterious effects of cardiac stress. These discoveries reveal a signaling pathway that transduces membrane stresses into transcriptome changes in the setting of E-C uncoupling following cardiac stress.

JP2 was initially discovered as a structural protein with dual membrane anchoring domains that connect T-tubules and the SR membrane.(8) Here we discovered that JP2 contains additional regulatory domains that extend beyond its role as a structural protein. An NLS in the N-terminal region of JP2 is necessary for nuclear import of the calpain-generated JP2NT truncate. Thus, under stress conditions, calpain-mediated cleavage of JP2 serves two purposes: 1) impairs the bridging of T-tubules with the SR membrane (contributing to cardiomyocyte ultrastructural remodeling and E-C uncoupling (23)); and 2) liberates JP2NT, allowing JP2NT to translocate to the nucleus and mediate transcriptional reprogramming. In addition, we found that the α-helix region of JP2 contains a previously unappreciated DNA binding domain that mediates selective binding to canonical TATA box motifs and MRE. This DNA binding domain is evolutionarily conserved, suggestive of a dual function for JP2 as a structural protein and transcriptional regulator in other species.

The development and progression of heart failure involves diverse cellular and molecular mechanisms (41, 42). Our ChIP-seq and transcriptomic profiling data suggest that JP2NT suppresses gene transcription by targeting multiple signaling pathways such as inflammatory responses, fibrosis, myocyte hypotrophy, and cell death among others. Taken with the protective effect of JP2NT overexpression in the setting of cardiac stress, this study indicates that JP2NT is an endogenous self-protective stress transducer that conveys the E-C uncoupling signal to the nucleus, regulates transcriptional reprogramming, and ultimately attenuates the progression of heart failure. As JP2 is abundant in all muscle cells (cardiac, skeletal and smooth muscle), JP2NT may serve as a general protective mechanism antagonizing stress-induced pathological remodeling related to many diseases.

Supplementary Material

Refer to Web version on PubMed Central for supplementary material.

Acknowledgments:

We thank M. J. Welsh, K. P. Campbell, E. D. Abel, B. London, L. Yang (University of Iowa) and S. R. Wayne Chen (University of Calgary) for reading the manuscript and constructive comments. The authors thank S. R. Ikeda (NIAAA/NIH) for providing TEVp plasmids.

Funding: This work was funded by NIH R01 HL090905, HL130346, VA 1I01BX002334 (L.S.S.), AHA 16SDG30820003 (A.G.), NIH R01HG008759 (K.F.A), NIH OD019941 (B.W.), NSF 81570293 (J.H.).

References and Notes

1. Clapham DE, Calcium signaling. Cell 131, 1047–1058 (2007). [PubMed: 18083096]
2. Bers DM, Cardiac excitation-contraction coupling. Nature 415, 198–205 (2002). [PubMed: 11805843]
3. Cheng H, Lederer WJ, Cannell MB, Calcium sparks: elementary events underlying excitation-contraction coupling in heart muscle. Science 262, 740–744 (1993). [PubMed: 8235594]
4. Cannell MB, Cheng H, Lederer WJ, The control of calcium release in heart muscle. Science 268, 1045–1049 (1995). [PubMed: 7754384]
5. Lopez-Lopez JR, Shacklock PS, Balke CW, Wier WG, Local calcium transients triggered by single L-type calcium channel currents in cardiac cells. Science 268, 1042–1045 (1995). [PubMed: 7754383]
6. Wang SQ, Song LS, Lakatta EG, Cheng H, Ca2+ signalling between single L-type Ca2+ channels and ryanodine receptors in heart cells. Nature 410, 592–596 (2001). [PubMed: 11279498]
7. Page E, Surdyk-Droske M, Distribution, surface density, and membrane area of diadic junctional contacts between plasma membrane and terminal cisterns in mammalian ventricle. Circ Res 45, 260–267 (1979). [PubMed: 376173]
8. Takeshima H, Komazaki S, Nishi M, Iino M, Kangawa K, Junctophilins: a novel family of junctional membrane complex proteins. Mol Cell 6, 11–22 (2000). [PubMed: 10949023]
9. Nishi M, Mizushima A, Nakagawara K, Takeshima H, Characterization of human junctophilin subtype genes. Biochem Biophys Res Commun 273, 920–927 (2000). [PubMed: 10891348]
10. van Oort RJ et al., Disrupted junctional membrane complexes and hyperactive ryanodine receptors after acute junctophilin knockdown in mice. Circulation 123, 979–988 (2011). [PubMed: 21339484]
11. Guo A et al., Overexpression of junctophidn-2 does not enhance baseline function but attenuates heart failure development after cardiac stress. Proc Natl Acad Sci USA 111, 12240–12245 (2014). [PubMed: 25092313]
12. Gomez AM et al., Defective excitation-contraction coupling in experimental cardiac hypertrophy and heart failure. Science 276, 800–806 (1997). [PubMed: 9115206]
13. Litwin SE, Zhang D, Bridge JH, Dyssynchronous Ca(2+) sparks in myocytes from infarcted hearts. Circ Res 87, 1040–1047 (2000). [PubMed: 11090550]
14. Song LS et al., Orphaned ryanodine receptors in the failing heart. Proc Natl Acad Sci U S A 103, 4305–4310 (2006). [PubMed: 16537526]
15. Xu M et al., Intermolecular failure of L-type Ca2+ channel and ryanodine receptor signaling in hypertrophy. PLoS Biol 5, e21 (2007). [PubMed: 17214508]
16. Guo A, Zhang C, Wei S, Chen B, Song LS, Emerging mechanisms of T-tubule remodelling in heart failure. Cardiovasc Res 98, 204–215 (2013). [PubMed: 23393229]
17. Wei S et al., T-tubule remodeling during transition from hypertrophy to heart failure. Circ Res 107, 520–531 (2010). [PubMed: 20576937]
18. Xu M et al., Mir-24 regulates junctophilin-2 expression in cardiomyocytes. Circ Res 111, 837–841 (2012). [PubMed: 22891046]
19. Wu HD et al., Ultrastructural remodelling of Ca(2+) signalling apparatus in failing heart cells. Cardiovasc Res 95, 430–438 (2012). [PubMed: 22707157]

20. Jiang M et al., JPH-2 interacts with Cai-handling proteins and ion channels in dyads: Contribution to premature ventricular contraction-induced cardiomyopathy. Heart Rhythm 13, 743–752 (2016). [PubMed: 26538326]
21. Minamisawa S et al., Junctophilin type 2 is associated with caveolin-3 and is down-regulated in the hypertrophic and dilated cardiomyopathies. Biochem Biophys Res Commun 325, 852–856 (2004). [PubMed: 15541368]
22. Zhang HB et al., Ultrastructural uncoupling between T-tubules and sarcoplasmic reticulum in human heart failure. Cardiovasc Res 98, 269–276 (2013). [PubMed: 23405000]
23. Wu CY et al., Calpain-dependent cleavage of junctophilin-2 and T-tubule remodeling in a mouse model of reversible heart failure. J Am Heart Assoc 3, e000527 (2014). [PubMed: 24958777]
24. Guo A et al., Molecular Determinants of Calpain-dependent Cleavage of Junctophilin-2 Protein in Cardiomyocytes. J Biol Chem 290, 17946–17955 (2015). [PubMed: 26063807]
25. Wang Y et al., Targeting Calpain for Heart Failure Therapy: Implications From Multiple Murine Models. JACC Basic Transl Sci 3, 503–517 (2018). [PubMed: 30175274]
26. Molkentin JD et al., A calcineurin-dependent transcriptional pathway for cardiac hypertrophy. Cell 93, 215–228 (1998). [PubMed: 9568714]
27. Frey N, McKinsey TA, Olson EN, Decoding calcium signals involved in cardiac growth and function. Nat Med 6, 1221–1227 (2000). [PubMed: 11062532]
28. Passier R et al., CaM kinase signaling induces cardiac hypertrophy and activates the MEF2 transcription factor in vivo. J Clin Invest 105, 1395–1406 (2000). [PubMed: 10811847]
29. Backs J, Song K, Bezprozvannaya S, Chang S, Olson EN, CaM kinase II selectively signals to histone deacetylase 4 during cardiomyocyte hypertrophy. J Clin Invest 116, 1853–1864 (2006). [PubMed: 16767219]
30. Wu X et al., Local InsP3-dependent perinuclear Ca2+ signaling in cardiac myocyte excitation-transcription coupling. J Clin Invest 116, 675–682 (2006). [PubMed: 16511602]
31. Colella M et al., Ca2+ oscillation frequency decoding in cardiac cell hypertrophy: role of calcineurin/NFAT as Ca2+ signal integrators. Proc Natl Acad Sci USA 105, 2859–2864 (2008). [PubMed: 18287024]
32. Houser SR, Molkentin JD, Does contractile Ca2+ control calcineurin-NFAT signaling and pathological hypertrophy in cardiac myocytes? Sci Signal 1, pe31 (2008). [PubMed: 18577756]
33. Galvez AS et al., Cardiomyocyte degeneration with calpain deficiency reveals a critical role in protein homeostasis. Circ Res 100, 1071–1078 (2007). [PubMed: 17332428]
34. Patterson C, Portbury AL, Schisler JC, Willis MS, Tear me down: role of calpain in the development of cardiac ventricular hypertrophy. Circ Res 109, 453–462 (2011). [PubMed: 21817165]
35. Williams DJ, Puhl HL, 3rd, Ikeda SR, Rapid modification of proteins using a rapamycin-inducible tobacco etch virus protease system. PloS one 4, e7474 (2009). [PubMed: 19830250]
36. Sigrist CJ et al., PROSITE: a documented database using patterns and profiles as motif descriptors. Brief Bioinform 3, 265–274 (2002). [PubMed: 12230035]
37. Narasimhan G et al., Mining protein sequences for motifs. J Comput Biol 9, 707–720 (2002). [PubMed: 12487759]
38. Wysocka J, Reilly PT, Herr W, Loss of HCF-1-chromatin association precedes temperature-induced growth arrest of tsBN67 cells. Molecular and cellular biology 21, 3820–3829 (2001). [PubMed: 11340173]
39. Sayed D, He M, Yang Z, Lin L, Abdellatif M, Transcriptional regulation patterns revealed by high resolution chromatin immunoprecipitation during cardiac hypertrophy. J Biol Chem 288, 2546–2558 (2013). [PubMed: 23229551]
40. Naya FJ, Wu C, Richardson JA, Overbeek P, Olson EN, Transcriptional activity of MEF2 during mouse embryogenesis monitored with a MEF2-dependent transgene. Development 126, 2045–2052 (1999). [PubMed: 10207130]
41. Mudd JO, Kass DA, Tackling heart failure in the twenty-first century. Nature 451, 919–928 (2008). [PubMed: 18288181]

42. van Berio JH, Maillet M, Molkentin JD, Signaling effectors underlying pathologic growth and remodeling of the heart. J Clin Invest 123, 37–45 (2013). [PubMed: 23281408]

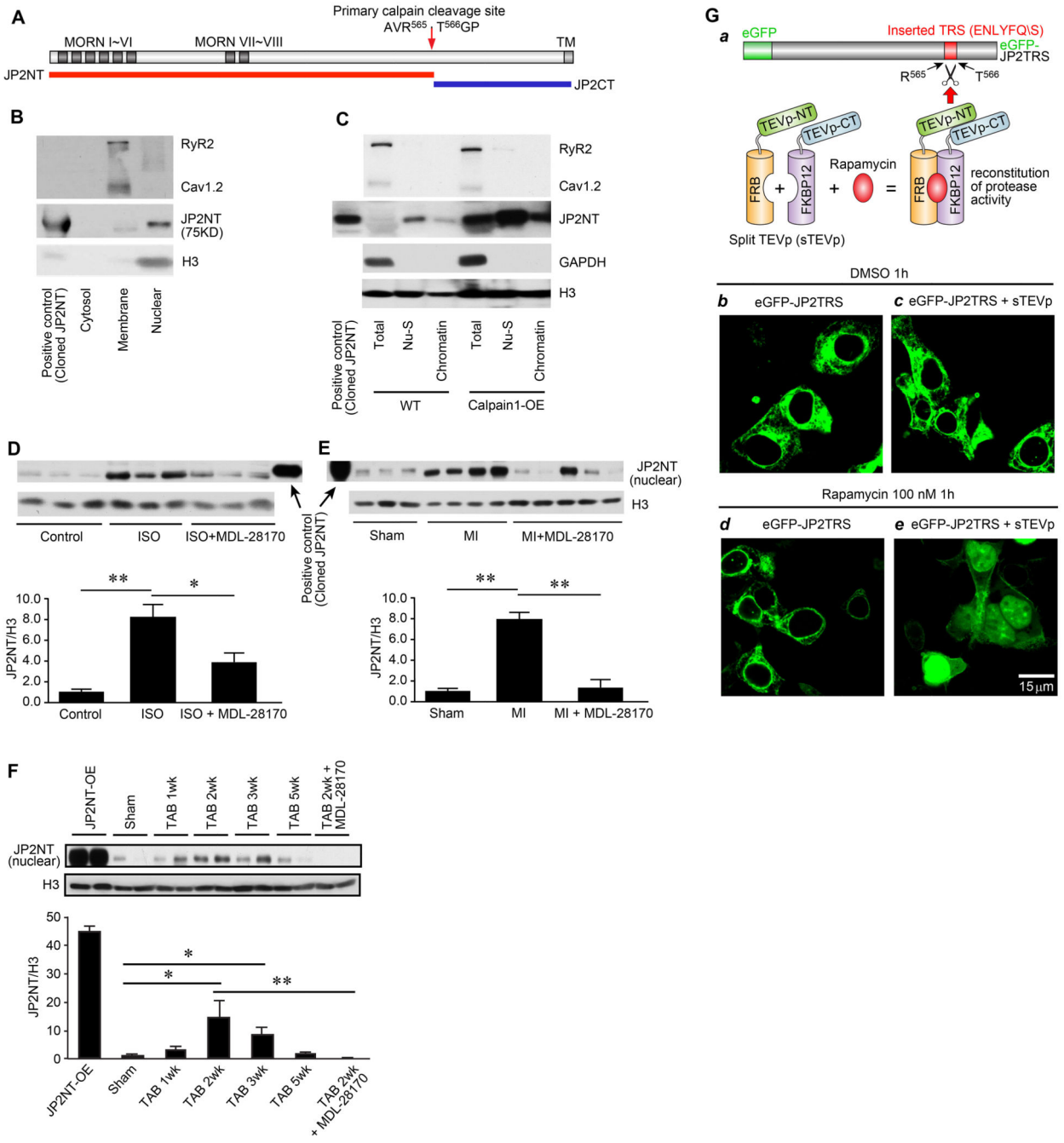

Fig. 1. JP2 N-terminal truncate (JP2NT) accumulates in the nucleus of stressed hearts.

(A) Schematic of JP2 and JP2 truncates. **(B)** JP2NT is primarily present in nuclear fractions of murine heart lysates. H3: Histone H3 (nuclear marker). $Ca_V1.2$: L-type Ca^{2+} channel (membrane marker). **(C)** Increased endogenous JP2NT in soluble (Nu-S) and chromatin-containing (chromatin) nuclear fractions from 3 weeks postnatal calpain 1-overexpressing (OE) hearts. The chromatin fraction was derived by treating chromatin pellet with micrococcal nuclease (MNASE), which cleaves DNA and releases chromatin-associated proteins (*see also Fig. 2C*). **(D-F)** Increased endogenous JP2NT levels in chronic cardiac

stress models: **(D)** isoproterenol (ISO, 1 week) minipump infusion; **(E)** myocardial infarction (MI, 1 week); **(F)** TAB-induced ventricular pressure overload. Calpain inhibitor MDL-28170 attenuated or abolished the elevation of nuclear JP2NT in all these models. JP2NT-OE: transgenic mouse with cardiac specific expression of JP2NT. The overexpression level of JP2NT is in the same order of magnitude of the peak level of endogenous JP2NT induced by TAB. N=3-4 for each group; * $p < 0.05$; ** $p < 0.01$ by t-test or Kruskal-Wallis rank test when appropriate. **(G)** Analysis of JP2NT nuclear translocation using the rapamycin-inducible split tobacco etch virus protease (sTEVp) system. ***a***, Schematic of the sTEVp system. The N- and C-terminal fragments of TEV protease were fused to FRB and FKBP12, respectively. Rapamycin induces reconstitution of TEV protease through the FKBP-rapamycin-FRB complex. A TEVp substrate recognition sequence (TRS) was inserted into the primary calpain cleavage site (R^{565}/T^{566}) of JP2 (eGFP-JP2TRS), allowing for inducible and site-specific rapid cleavage of substrates at the TRS. ***b-e***, eGFP-JP2TRS was transfected into HEK293T cells alone (*b, d*) or with sTEVp system (*c, e*), followed by treatment with DMSO control (*b, c*) or rapamycin (100 nM) for 1 hr (*d, e*).

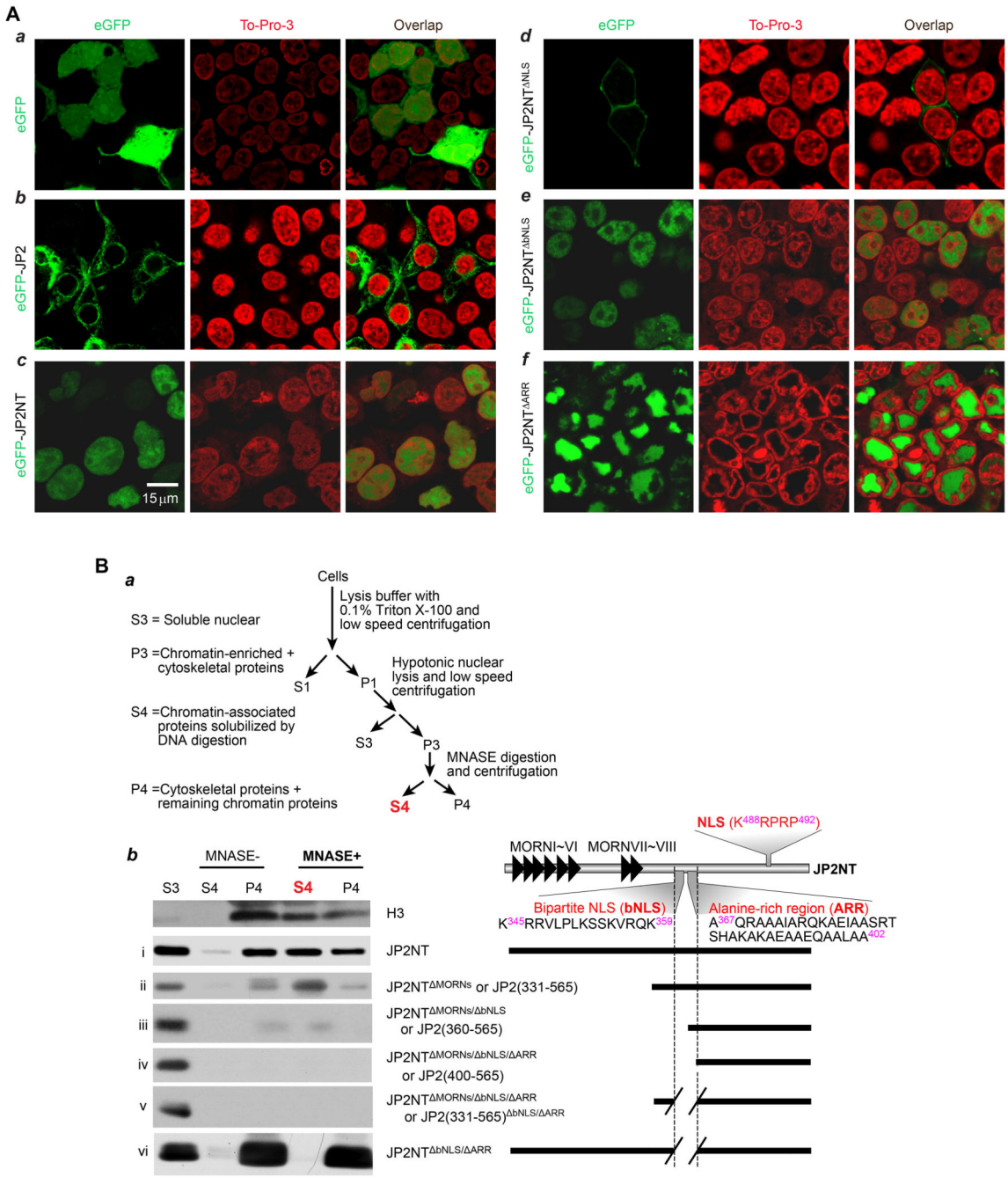

Fig. 2. JP2NT contains a NLS and a chromatin/DNA-binding domain.

(A) A conserved NLS is essential for nuclear accumulation of JP2NT. ***a-c***, Subcellular localization of eGFP and eGFP-fused JP2 and eGFP-JP2NT in HEK293T cells. Full length JP2 localizes on both plasma membrane and ER network (***b***). JP2NT is highly enriched in nuclei (***c***). ***d***, Deletion of NLS from JP2NT (JP2NT$^{\Delta NLS}$) abolished its nuclear localization and restricted its localization on plasma membrane, ***e-f***, A domain containing a bipartite NLS (bNLS) and an alanine-rich region (ARR) is essential for co-localization of JP2NT with DNA (stained with To-Pro-3). eGFP-fused JP2NT mutants without the bNLS

(JP2NT$^{\Delta bNLS}$, ***e***) or without the alanine-rich domain (JP2NT$^{\Delta ARR}$, ***f***) lost co-localization with DNA. **(B)** JP2NT associates with chromatin. ***a***, Schematic of the subcellular fractionation approach (adapted from *Wisoka et al* 2001). ***b***, Subnuclear distribution of JP2NT and fragments/mutants. JP2NT is present in both soluble nuclear (S3) and MNASE-releasable chromatin fractions (S4+MNASE). Deletion of the MORN domains (JP2NT$^{\Delta MORNs}$) had no effect on subnuclear distribution of JP2NT. However, the amount of chromatin-associated JP2NT was decreased by deletion of the bNLS alone (JP2NT$^{\Delta MORNs/\Delta bNLS}$). or deletion of both the bNLS and ARR (JP2NT$^{\Delta MORNs/\Delta bNLS/\Delta ARR}$ and JP2NT$^{\Delta bNLS/\Delta ARR}$). Histone H3: chromatin marker.

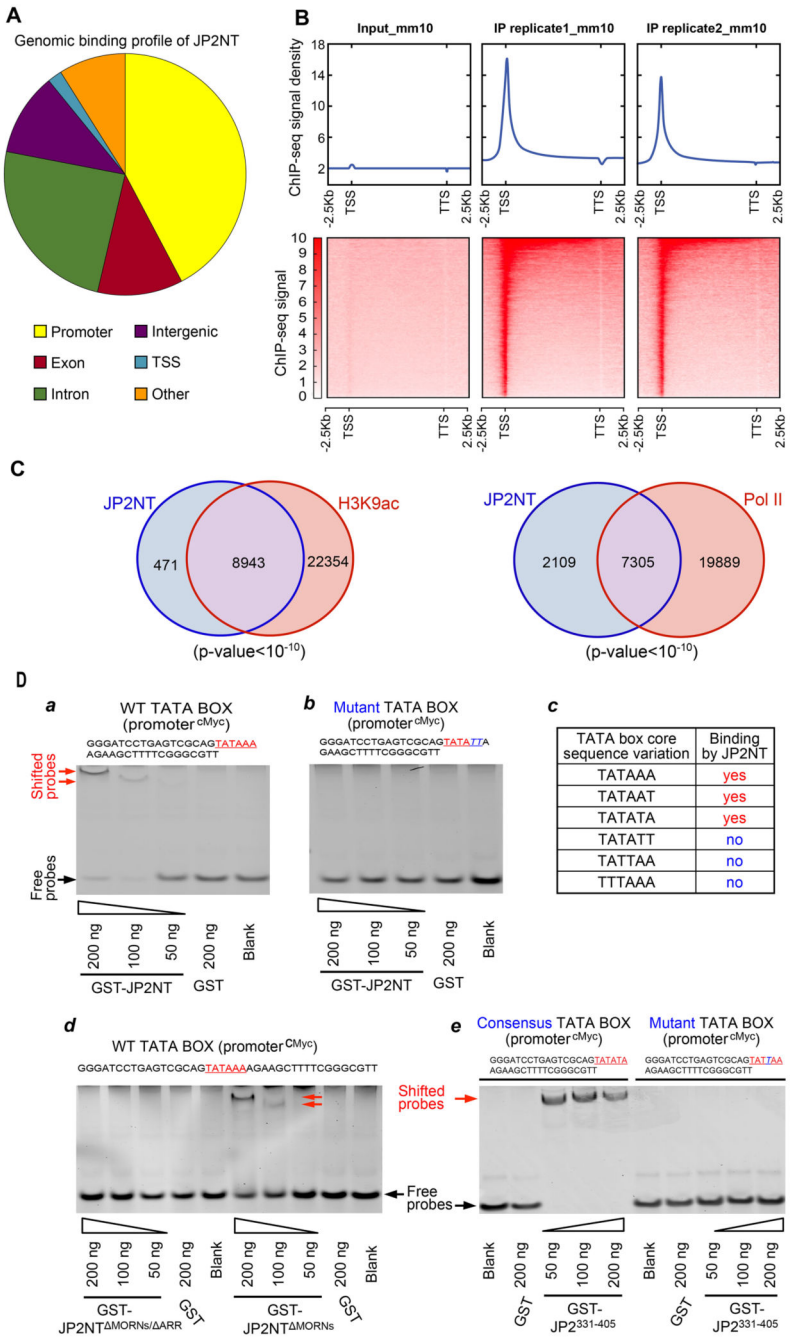

Fig. 3. JP2NT is a TATA-box binding protein enriched at transcription start site (TSS) and interacts with basic transcription machinery.

(A) Genomic DNA binding profile of JP2NT in cardiomyocytes as revealed by ChIP-seq. **(B)** JP2NT is preferentially localized around TSS as revealed by two replicates of ChIP-seq. **(C)** Overlap chart of DNA binding peaks of indicated proteins. **(D)** JP2NT binds to TATA box DNA sequences *in vitro*. ***a-b***, Gel shift assays of purified GST-JP2NT binding to WT (*a*), or mutant TATA box-containing sequences (*b*) derived from the cMyc promoter, ***c***, Summary of the results of gel shift assays with various of TATA box variants or mutants.

Mutation of the core TATA sequences abolished the interaction with GST-JP2NT. ***d***, Deletion of the ARR, but not the N-terminal MORN domains, eliminated JP2NT binding to the TATA box sequence. ***e***, The peptide $JP2^{331-405}$ containing the ARR specifically binds to WT TATA box sequence.

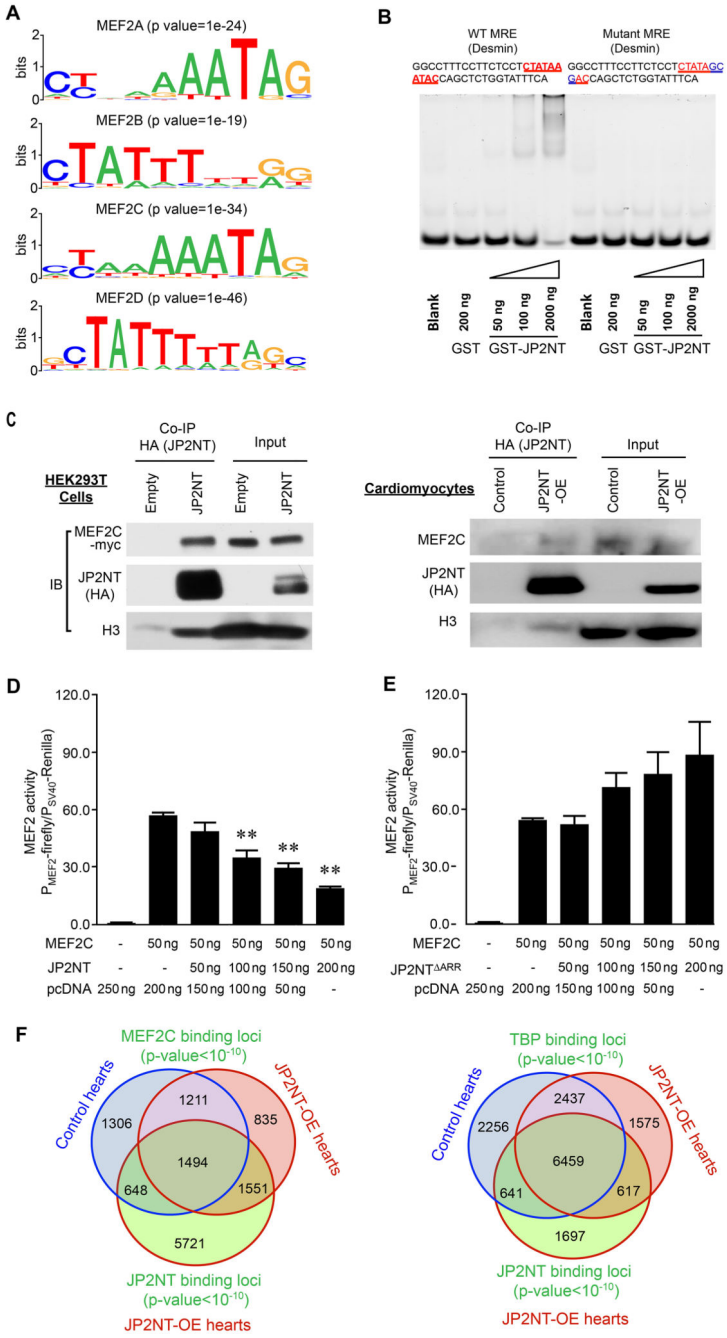

Fig. 4. JP2NT represses MEF2-mediated transcription by competing for the MEF2 Response Element (MRE).

(A) Enrichment of MEF2 binding motifs in ChIP-seq dataset. **(B)** Gel shift assay of JP2NT binding to a desmin enhancer-derived DNA sequence containing a WT or mutant MRE *in vitro*. **(C)** Co-immunoprecipitation of HA-tagged JP2NT binding to MEF2C or Histone H3 in HEK293T cells transfected with JP2NT and MEF2C as well as in JP2NT-OE hearts (postnatal 2 weeks). (**D & E**) MEF2 activity assays in HEK293T cells co-transfected with P_{MEF2}-firefly, P_{SV40}-renilla, MEF2C and WT JP2NT (D) or a mutant lacking the ARR (E,

JP2NT$^{\Delta ARR}$). n≥3 independent batches of experiments, 3 transfection replicates for each batch of experiment. ** $p < 0.01$ vs. MEF2C+empty pcDNA . **(F)** Overlap chart of MEF2 (left) and TBP (right) DNA binding peaks compared between control and JP2NT-OE hearts, as well as compared with JP2NT binding peaks from JP2NT-OE hearts.

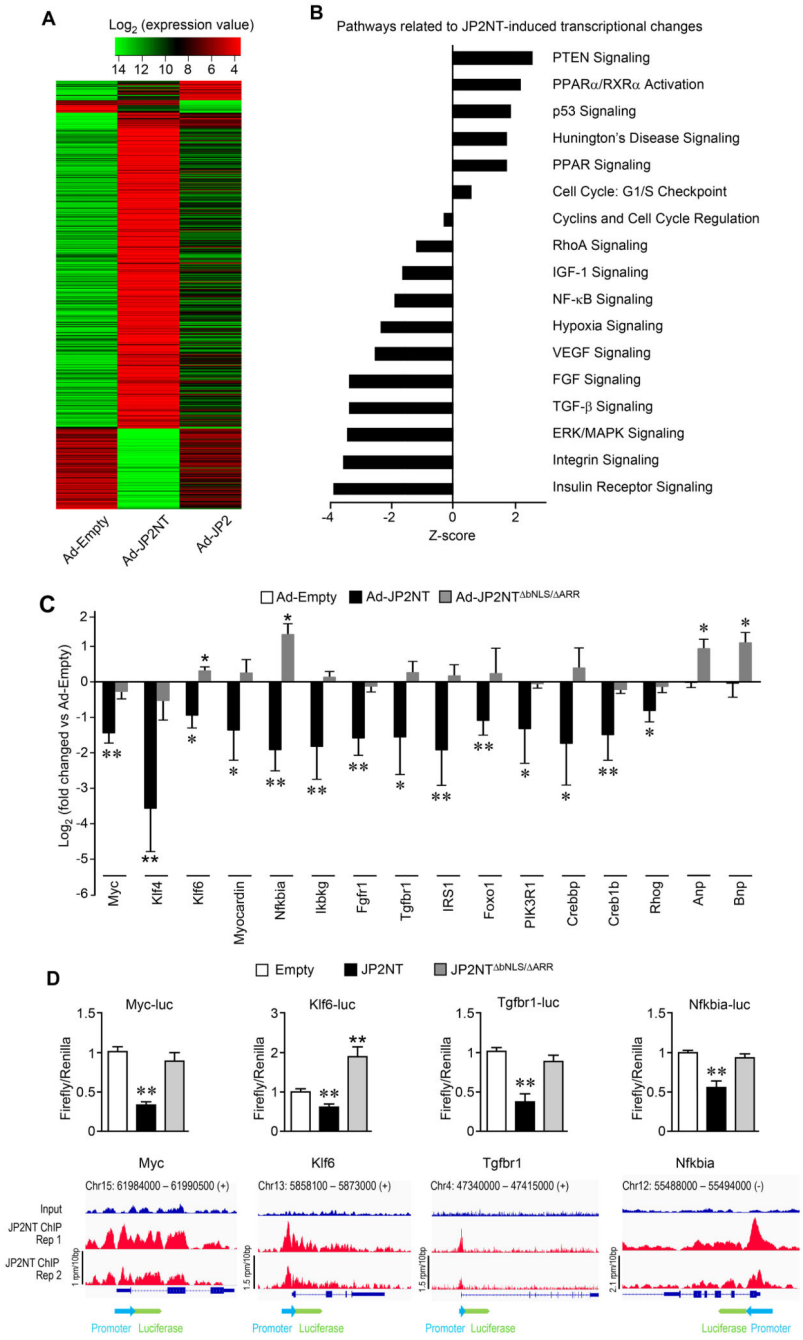

Fig. 5. JP2NT drives broad-spectrum transcriptional reprogramming in cultured cardiomyocytes.

(A) Heatmap of significantly altered genes in cultured adult murine cardiomyocytes expressing JP2 or JP2NT by adenovirus (Ad). **(B)** IPA pathway enrichment analysis of significantly altered transcripts induced by JP2NT. **(C)** RT-qPCR validation of genes that were significantly down-regulated by JP2NT as compared to Ad-Empty control. Note that deletion of the ARR (JP2NT$^{\Delta ARR}$) prevented JP2NT-mediated transcriptional repression. Data were calculated as the Log2 fold change relative to cells transfected with Ad-Empty.

Each transcript was assayed in n≥4 batches of cells. **(D)** Transcriptional activity assays in which luciferase is under the control of the indicated promoters. n≥3 independent batches of HEK293T cells, 3 transfection replications included in each batch; *, $p<0.05$, ** $p < 0.01$ vs. control (empty virus or plasmid). Under each bar graph are the JP2NT binding tracks at these gene loci and location of cloned promoters for luciferase construct, respectively.

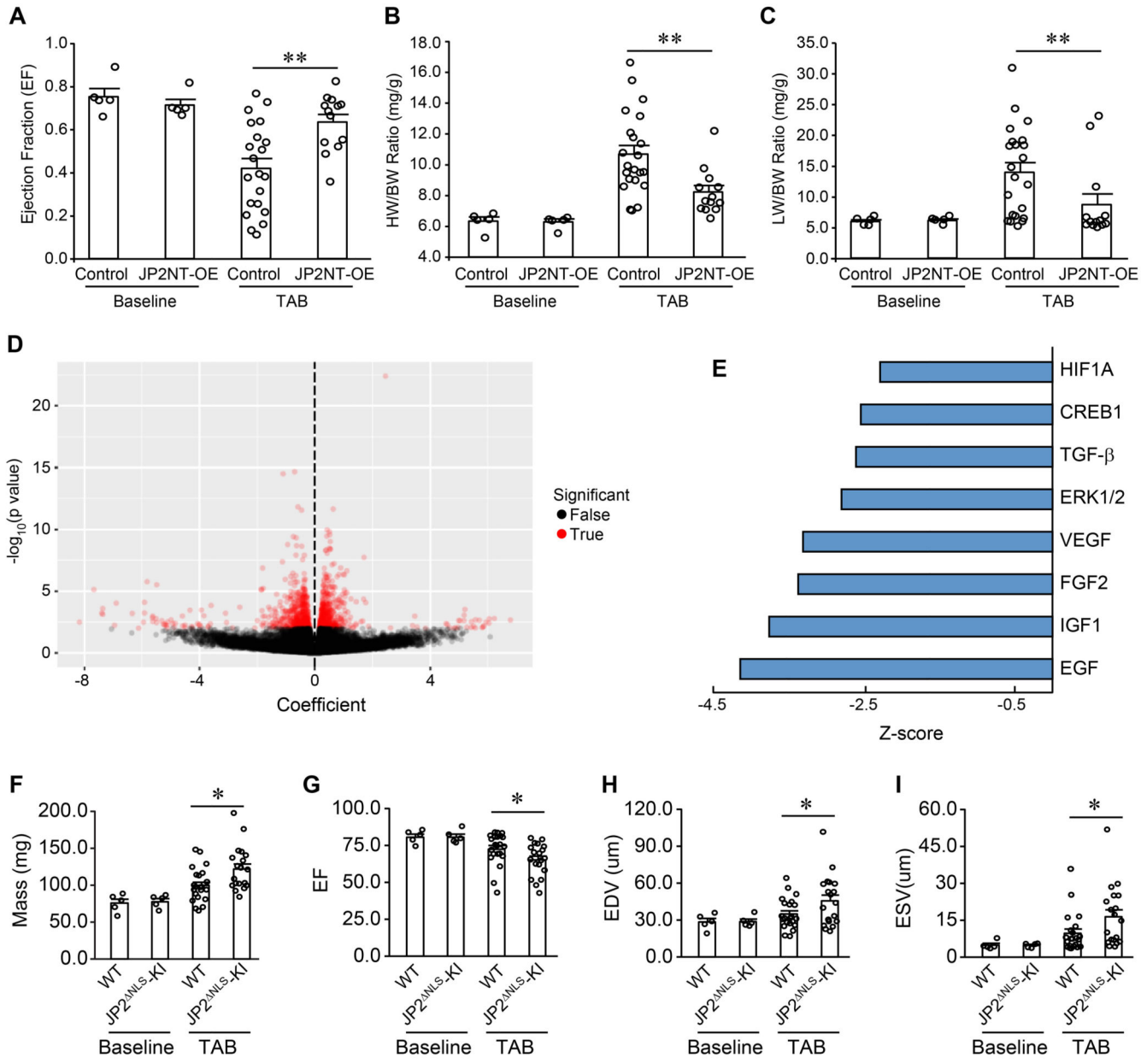

Fig. 6. JP2NT overexpression protects against pressure overload-induced hypertrophy and heart failure.

(A) Cardiac specific overexpression of JP2NT (JP2NT-OE) preserved cardiac ejection fraction (EF) in mice 3 weeks after transverse aortic banding (TAB). **(B)** JP2NT overexpression attenuated TAB-induced cardiac hypertrophy as evidenced by a decreased heart weight/body weight (HW/BW) ratio. **(C)** Lung weight/body weight (LW/BW) ratio is significantly reduced in JP2NT-OE mice following TAB. n=5, 5, 22, 13 for each group respectively. **(D)** Volcano plot of the effect of JP2NT overexpression on TAB-induced transcriptional remodeling. JP2NT-OE significantly changed the transcriptional response to TAB. Red dots indicate the transcripts whose response to TAB was significantly changed by JP2NT-OE. **(E)** IPA pathway enrichment analysis of significantly altered transcripts in

JP2NT-OE mice following TAB as compared to littermate controls. **(F-I)** Echocardiogram measurement of heart mass **(F)**, ejection fraction **(G)**, EDV **(H)** and ESV **(I)** in WT and $JP2^{\Delta NLS}$-KI mice under baseline or TAB condition.